HAL open science

# p722 ferrocifen loaded lipid nanocapsules improve survival of murine xenografted-melanoma via a potentiation of apoptosis and an activation of CD8+ T lymphocytes

Solène Topin-Ruiz, Adélie Mellinger, Elise Lepeltier, Clara Bourreau, Juliette Fouillet, Jeremie Riou, Gérard Jaouen, Ludovic Martin, Catherine Passirani, Nicolas Clere

## To cite this version:

Solène Topin-Ruiz, Adélie Mellinger, Elise Lepeltier, Clara Bourreau, Juliette Fouillet, et al.. p722 ferrocifen loaded lipid nanocapsules improve survival of murine xenografted-melanoma via a potentiation of apoptosis and an activation of CD8+ T lymphocytes. International Journal of Pharmaceutics, 2021, 593, pp.120111. 10.1016/j.ijpharm.2020.120111 . hal-03026310

**HAL Id: hal-03026310**

**https://hal.science/hal-03026310**

Submitted on 15 Dec 2022

**HAL** is a multi-disciplinary open access archive for the deposit and dissemination of scientific research documents, whether they are published or not. The documents may come from teaching and research institutions in France or abroad, or from public or private research centers.

L'archive ouverte pluridisciplinaire **HAL**, est destinée au dépôt et à la diffusion de documents scientifiques de niveau recherche, publiés ou non, émanant des établissements d'enseignement et de recherche français ou étrangers, des laboratoires publics ou privés.

Distributed under a Creative Commons Attribution - NonCommercial 4.0 International License

Version of Record: https://www.sciencedirect.com/science/article/pii/S0378517320310966
Manuscript_778504229f78d10aa6bc68b169d5bcf4

# p722 ferrocifen loaded lipid nanocapsules improve survival of murine xenografted-melanoma *via* a potentiation of apoptosis and an activation of CD8$^+$ T lymphocytes

Solène Topin-Ruiz[1,2*], Adélie Mellinger[1*], Elise Lepeltier[1], Clara Bourreau[1], Juliette Fouillet[1], Jérémie Riou[1], Gérard Jaouen[3,4], Ludovic Martin[2], Catherine Passirani[1], Nicolas Clere[1]

(1) MINT, Univ Angers, INSERM, CNRS, IBS-CHU, 4 rue Larrey, F-49933 Angers, France
(2) Centre Hospitalier Universitaire, service de dermatologie, 4 rue Larrey, F-49933 Angers, France
(3) PSL, Chimie ParisTech, Paris Cedex 05, France
(4) Sorbonne Université, CNRS, Institut Parisien de Chimie Moléculaire (IPCM, UMR 8232), Paris Cedex 05, France

(*) These authors contributed equally

Conflicts of interest: None

**Corresponding author**
Nicolas CLERE – Pharm D., Ph D
UMR Inserm 1066 – CNRS 6021
IBS – IRIS
CHU
4, rue Larrey
F-49933 ANGERS Cedex
nicolas.clere@univ-angers.fr

Word numbers: Abstract (177 words); Text (5,912 words);

References (41);

Number of Figures (6); Number of table (1)



© 2020 published by Elsevier. This manuscript is made available under the CC BY NC user license
https://creativecommons.org/licenses/by-nc/4.0/

31 **Table of abbreviations**

32 **AUC :** Area under the curve

33 **Bax :** Bcl2-associated protein X

34 **BCl-2 :** B-cell lymphoma 2

35 **CTLA-4 :** Cytotoxic T-lymphocyte associated protein 4

36 **DMSO :** Dimethyl-sulfoxide

37 **DSPE-PEG :** 1, 2-Distearoyl-sn-glycero-3-phosphoethanolamine-Poly(ethylene glycol)

38 **HBSS :** Hank's Balanced Salt Solution

39 **LNC :** Lipid nanocapsules

40 **mAb :** Monoclonal antibody

41 **MeOH :** Methanol

42 **MEK :** Mitogen-activated extracellular signal-regulated protein kinase

43 **NaCl :** Sodium chloride

44 **PBS :** Phosphate buffered saline

45 **PD-1 :** Programmed cell death protein 1

46 **PEG :** Polyethylene glycol

47 **PdI :** Polydispersity index

48 **ROS :** Reactive oxygen species

49 **RPMI :** Roswell Park Memorial Institute medium

50 **UPLC :** Ultra Performance Liquid Chromatography

51

52 **Highlights**

53 - p722-LNC induces a significant decrease of B16F10 melanoma cell viability
54 - p722-LNC slows tumor growth and improves the survival of treated mice
55 - Antitumor activities of p722-LNC are explained by a potentiation of intrinsic
56 apoptotic pathway and an activation of $CD8^+$ T lymphocytes

57

**Abstract**

Metastatic melanoma is a malignant tumor with a poor prognosis. Recent new therapeutics improved the survival of patients at a metastatic stage. However, the low response rate to immunotherapy, explained in part by resistance to apoptosis, needs to develop new strategies. The ferrocifen family represents promising bioorganometallic molecules for melanoma treatment since they show potent anticancer properties. The aim of this study is (i) to evaluate the benefits of a strategy involving encapsulated p722 in lipid nanocapsules (LNC) in B16F10 melanoma mice models and (ii) to compare the beneficial effects with an existing therapy such as anti-CTLA4 mAb. Interestingly, LNC-p722 induces a significant decrease of melanoma cell viability. *In vivo* data shows a significant improvement in the survival rate and a slower tumor growth with p722-loaded LNC in comparison with anti-CTLA4 mAb. Western blots confirm that LNC-p722 potentiates intrinsic apoptotic pathway. Treatment with LNC-p722 significantly activates $CD8^+$ T lymphocytes compared to treatment with anti-CTLA4 mAb. This study uncovers a new therapeutic strategy with encapsulated p722 to prevent B16F10 melanoma growth and to improve survival of treated mice.

**Keywords:** Ferrocifen, metastatic melanoma, CD8 T lymphocytes, apoptosis

## Introduction

Cutaneous cancers are among the most common cancers, with more than two to three million new cases around the world each year. The incidence of melanoma increased dramatically over the past 50 years [1]. Although it accounts for 5% of all skin cancers, cutaneous melanoma is responsible for 75% of skin cancer deaths. The survival rate of melanoma varies depending on the stage of the disease at the time of prognosis. Thus, overall relative survival rate at any stage is 97% at one year, 85% at five years while, in metastatic conditions, the median survival is six to nine months.

Where melanoma is concerned, the difficulties of early dissemination and pronounced chemotherapy resistance remained completely unsolved for decades [2]. Since 2011, the situation has improved due to the development of new targeted therapies such as BRAF or MEK inhibitors and efficient immune-stimulating antibodies such as anti-CTLA4, anti-PD1 or anti-PDL1. Several mechanisms have been linked to CTLA4-mediated activities [3]. During native T cell activation, the expression of CTLA4 protein on the cell surface is upregulated and directly competes with the CD28 protein in binding with the CD80 and CD86 molecules [4]. The inhibitory signals from CTLA4 can also prevent the activation of self-reactive T cells by attenuating T cell signaling. These strategies lead to a significant increase in metastatic melanoma patients‘overall survival time [5;6]. Nevertheless, for many patients, tumor relapses and therapy resistance often follow within only a few months or years, after an initial tumor reduction phase [7;8]. Thus, new therapeutic strategies are still needed, which may further improve the clinical outcome. Many drug candidates have been investigated and metal-based drugs, particularly ferrocifen-based drugs, represent a promising family of anticancer compounds [9;10].

99 The bioorganometallic molecules are active molecules containing at least one carbon atom
100 directly bound to a metal or metalloid. In ferrocifens, the metal studied is iron and the
101 metallocene derivative is ferrocene chemically grafted onto a polyphenolic skeleton,
102 resulting in ferrocenyl phenol derivatives [11]. In recent years, our group has demonstrated,
103 through tumor-xenografted mice model, the beneficial effects of ferrociphenol on the tumor
104 cell apoptosis or senescence in triple negative breast cancer [12] or in melanoma [10].
105 Furthermore, cytotoxic properties of ferrocifens have been reported through an increase in
106 the production of reactive oxygen species (ROS) [13] and the generation of an active redox
107 metabolite that interact selectively with nucleophilic biomolecules such as glutathione or
108 the thioredoxin reductase. However, due to their hydrophobicity, the use of lipid core
109 vectors such as lipid nanocapsules (LNC), allows an optimal encapsulation and an
110 intravenous administration of these molecules [14].
111 Among the therapeutic strategies for melanoma, immunotherapy has a key role for several
112 years. Thus, a significant improvement of the median overall survival has been observed
113 after treatment with ipilimumab, a monoclonal antibody against cytotoxic T-lymphocyte
114 antigen-4 (CTLA-4), which is able to exploit the natural ability of the immune system to
115 eradicate primary cancer cells [7]. Furthermore, it has been reported the benefit of the
116 combination of anti-CTLA4 antibodies and radiotherapy in metastatic melanoma. Thus, a
117 median survival prolongation of 3 to 5 months and response rates of 25.7 *vs* 6.5% have been
118 observed in anti-CTLA4 groups [15]. Taken together, these studies confirm the interest of
119 using anti-CTLA4 antibodies to treat metastatic melanoma.
120 The aim of this study was to evaluate the benefits of a strategy involving encapsulated p722
121 in LNC in B16F10 melanoma mice models. For the first time, an increase in therapeutic
122 efficacy was observed in LNC-p722 treated mice in comparison with anti-CTLA mAb treated

123 mice. Interestingly, LNC p722 is able to improve survival of murine xenografted-melanoma
124 *via* a potentiation of apoptosis and an activation of $CD8^+$ T lymphocytes
125
126 **Materials and methods**
127 **Chemical materials**
128 p722 (Fig. 1) was synthesized according to the protocol from Pigeon *et al*. [16]. The lipophilic
129 Labrafac® WL1349 (caprylic-capric acid triglycerides) was purchased from Gatefossé S.A.
130 (Saint-Priest, France). Lipoid® S75-3 (soybean lecithin at 69% of phosphatidylcholine came
131 from Lipoid GmbH (Ludwigshafen, Germany), Kolliphor®HS15 is a mixture of polyglycol
132 mono- and di-esters of 12-hydroxystearic acid and of about 30% of free polyethylene glycol
133 (BASF, Ludwigshafen, Germany), and NaCl from Prolabo (Fontenay-sous-bois, France).
134 Deionised water was acquired from Milli-Q system (Millipore, Paris, France). DSPE-
135 mPEG2000 (Mean Molecular Weight, MMw = 2805 $g.mol^{-1}$) was provided by Avanti Polar
136 Lipids (Alabaster, USA).
137
138 **Formulation of p722-loaded lipid nanocapsules (p722-LNC)**
139 The LNC vehicle was formulated in accordance with a phase inversion method, as previously
140 described[17]. Firstly, all the excipients were mixed (16.9% w/w Kolliphor®HS15 (BASF,
141 Ludwigshafen, Germany), 1.5% w/w Lipoid®S75-3 (Lipoid GmbH, Ludwigshafen, Germany),
142 20.6% w/w Labrafac® (caprylic-capric acid triglycerides, Gatefossé S.A. Saint-Priest, France),
143 1.8% w/w NaCl (Prolabo, Fontenay-sous-Bois, France) and 59.2% w/w water (obtained from
144 a Milli-Q system, Millipore, Paris, France)) under magnetic stirring and heated from room
145 temperature to 60°C for 15 min. Three temperature cycles between 60 and 90 °C were
146 performed to obtain phase inversions of the emulsion. Secondly, when the temperature was

147 in the phase inversion zone (73-78°C), ice-cold water was added (88.4%v/v) to induce
148 irreversible shock and dilution, and to form the LNC suspension. The nanocapsules were
149 stored at 4°C. To formulate p722-LNC, 0.5% w/w p722 powder (concentration at 2.35 mM)
150 was added at step I, with all the excipients and the formulation process was the same as for
151 empty LNC. To separate free p722 from p722-loaded lipid nanocapsules, the suspension was
152 passed through 0.2 µm cellulose acetate filter.
153
154 *Post-insertion of DSPE-PEG*
155 The polymer used for post-insertion was 1,2-distearoyl-sn-glycero-3-phosphoethanolamine-
156 N- [methoxy(polyethyleneglycol)-2000] (DSPE-mPEG2000) (Avanti Polar Lipids, Inc,
157 Alabaster, USA). DSPE-mPEG2000 and LNC were co-incubated for 4h at 37 °C, with a final
158 polymer concentration adjusted to 5 mM. At this concentration, the post-insertion is total
159 [18] and the number of DSPE-mPEG2000 molecules per LNC is around 3 [19].
160
161 *Characterization of p722-LNC: size and zeta potential*
162 The mean diameter and polydispersity index (PdI) of LNC were characterized by using
163 Dynamic Light Scattering (DLS) from a Malvern Zetasizer® apparatus (Nano Series ZS,
164 Malvern Instruments S.A., Worcestershire, UK) at 25 °C, after dilution by 100 with UPW. The
165 measured average values were calculated from 3 runs, with 10 measurements per run.
166 The zeta potential of the nanocapsules was determined by laser Doppler micro-
167 electrophoresis using a Zetasizer Nano ZS system (Nano Series ZS, Malvern Instruments S.A.,
168 Worcestershire, UK) [20].
169
170 *Characterization of p722-LNC: encapsulation efficiency (EE)*

171 The encapsulated p722 concentration was directly measured by quantifying p722 in the LNC
172 using a supplier recommended UPLC method (Waters, France). For this purpose, the LNCs
173 were broken via a dilution by 10 in methanol (VWR international, Fontenay-sous-bois,
174 France). A BEH C18 analytical column (2.1 x 50 mm, 1.7 µm, Waters, France) was used at
175 room temperature. DMSO (Thermofisher, Kandel, Germany) and MeOH were used as mobile
176 phases (isocratic mode: 10:90, 10 min). The flow rate was 0.2 $mL.min^{-1}$, injection volume was
177 2 µL and p722 was quantified by a UV detector at a wavelength of 450 nm. Analysis of the
178 data was performed by Empower 3 software (Waters). Calibration curves were established
179 by quantifying the area under the curves (AUCs) of 0-200 $\mu g.mL^{-1}$ solutions of p722 in DMSO
180 and MeOH 10:90.
181
182 Encapsulation efficiency, EE (%), was calculated using the following equation:

183 $$EE\ (\%) = \frac{(Encapsulated\ p722\ conc.\ in\ LNC)\ \times\ 100}{Initial\ p722\ conc.\ in\ LNC}$$

184 Drug loading, DL (% w/w), was calculated using the following equation:

185 $$Drug\ loading\ (\%\ w/w)$$

186 $$= \frac{(Mass\ of\ encapsulated\ p722\ in\ 1\ mL\ of\ LNC\ dispersion)\ \times 100}{Total\ mass\ of\ excipients\ and\ p722\ in\ 1\ mL\ of\ LNC\ dispersion}$$

187
188 **Cell culture**
189 B16F10 mouse melanoma cell lines (gift from University of Brussels) were grown in RPMI-
190 1640 medium (Lonza, Verviers, Belgium) supplemented with 10% fetal bovine serum
191 (Biowest, Nuaillé, France), 1% non-essential amino acid (Lonza, Walkersvill, USA), 10 units of
192 penicillin and 10 mg of streptomycin (Sigma-Aldrich, Saint Louis, USA). B16F10 was cultured
193 according to ATCC protocol and maintained at 37°C in a humidified atmosphere with 5% $CO_2$.

194 **Determination of cell viability**

195 B16F10 cells were seeded onto 96-well plates at a density of $5x10^4$ cells/well and
196 precultured overnight. Cells were treated with p722, empty PEG-LNC ("blank") and p722
197 PEG-LNC for 24 h at a concentration range from $10^{-4}$ to 100 mg/mL[10]. Cytotoxicity tests
198 were performed using the MTT assay. The OD was evaluated by Multiskan Ascent
199 (Labsystems, Fischer Scientific, Wilmington, USA) at 492 nm.

200

201 ***In vivo* tumor development**

202 *Ethical approval*

203 All procedures involving animals, including the breeding protocols, were conducted in
204 accordance with protocols approved by the ethical committee of the University of Angers
205 and the regional ethics committee on animal testing (APAFIS#6540-2017012017467029v1).
206 Furthermore, animal experiments were carried out in strict accordance with
207 recommendations in the guidelines of the Code for Methods and Welfare Considerations in
208 Behavioral Research with Animals (Directive 2010/63/UE).

209

210 *Orthotopic model of B16F10 melanoma*

211 C57BL/6 mice were housed at the university animal facility (Service Commun d'Animalerie
212 Hospitalo-Universitaire; Université d'Angers, France) and were distributed in cages (4
213 mice/cages). A syngenic, allograft model of melanoma was obtained by subcutaneously
214 injecting a suspension of $10^6$ B16F10 melanoma cells in 100 µL of HBSS with calcium and
215 magnesium (Lonza, Walkersvill, Etats-Unis) into the right flank of mice. Before injecting cells,
216 mice were anesthetized with isoflurane (isoflurane was chosen because it induced rapid and
217 reversible anesthesia). Tumor size and tumor volume were monitored until the end of the

218 protocol and have been estimated using the formula: $V=\pi/6 \times L \times W^2$ (L: length and W:
219 Width). When the tumor volume was approximately 100 $mm^3$, mice were treated according
220 to the following protocol.
221 The treatment of mice was randomized and was administrated blind. When tumor volume
222 was around 100 $mm^3$ (day 0), mice were treated, with intraperitoneal injections of PEG-
223 p722-LNC (7 mg/kg) – to limit the first-pass hepatic effect - or blank PEG-LNC, daily from day
224 1 to day 5 at the beginning of the afternoon. Otherwise, mice were treated with anti-CTLA4
225 monoclonal antibody (10 mg/kg) on days 2, 4 and 6. At the end of the protocol, mice were
226 sacrificed (animals were anesthetized with isoflurane and then, euthanized by $CO_2$), and
227 tumors were removed, frozen and stored at -80°C. In accordance with ethical rules, the
228 animals were sacrificed when the tumor volume was greater than 2500 $mm^3$ or when the
229 animals showed signs of suffering.
230
231 **Western blot**
232 For the *in vitro* protocol, proteins were extracted from cells by scrapping with a cell lysis
233 buffer (10 mmol/L Tris-Base, 1 mmol/L $Na_3O_4$ and 1% SDS, pH 7.4). For the *in vivo* protocol,
234 mice tumors were grinded with Ultra-turrax in the same lysis buffer. Twenty micrograms of
235 proteins were resolved in 10% (*v*/*v*) SDS-PAGE gel and transferred onto a nitrocellulose
236 membrane (0.45 µm pore size) (Amersham GE Healthcare). Mouse anti-Bcl-2 (ab694,
237 Abcam) and rabbit anti-Bax (ab32503, Abcam), anti-Procaspase 9 (ab138412, Abcam), anti-
238 Caspase 9 (ab 202068, Abcam), anti-Procaspase 3 (ab 183179, Abcam) and anti-caspase 3 (ab
239 184787, Abcam) were used as primary antibodies. A second mouse (goat anti-mouse IgG,
240 secondary antibody, HRP conjugate, Life Technologies) and rabbit (61-6520, Invtrogen)
241 antibodies were used. Detection (using LAS4000, GE HealthCare) was performed using

242 enhanced chemoluminescence (ECL; Fisher Scientific, Pierce). In each case, protein levels
243 were normalized to the housekeeping protein actin and the protein expression fold
244 differences, between treated and control conditions, were plotted by ImageJ software.
245
246 **Immunophenotyping of mice lymphocytes**
247 To analyze the composition of mouse lymphocytes, blood samples were collected on days 1
248 and 9 (from the venous sinus) and at the end of the protocol (from a cardiac puncture). They
249 were diluted into a staining buffer (PBS, pH 7.0 plus 1% fetal calf serum) and cells were
250 stained with fluorescent-label CD3, CD8 and CD69 antibodies (BD Biosciences) for 45 min on
251 ice, followed by two washes in the staining buffer. Then, the cells were subjected to flow
252 cytometry analyses (PACEM platform, SFR ICAT, University of Angers, Angers, France).
253
254 **Statistical analysis**
255 Results were expressed as a median. For the *in vitro* study, statistical significance between
256 control and treated groups was evaluated using a Mann-Whitney test.
257 For the *in vivo* study, the statistical tests were performed with the R software. The tumoral
258 growth analysis was performed thanks to a linear mixt model (longitudinal data), including
259 the time influence (intra and inter day variability) and random intercept (intra and inter
260 individual variability). In order to obtain a reliable statistical model, the tumoral volume was
261 converted into a decimal logarithmic scale. Survival analysis was done using a log rang model
262 to compare survival curves and to calculate survival medians.
263 The significance threshold was defined at $p$ value $\leq 0.05$ for each statistical test.
264
265

266 **Results**

267 *Physico-chemical properties of lipid nanocapsules*

268 The p722 concentration into LNC was settled at 2.35 nM. At this concentration, the
269 encapsulation efficiency was 65% and the drug loading reached 0.7%. Hydrodynamic
270 diameter and zeta potential of the LNC suspensions are summarized in Table 1. The p722
271 entrapment into LNC did not modify the diameter compared to empty LNC. The size of
272 PEGylated LNC (unloaded or loaded with p722) showed a increase (of around 20 nm),
273 attributed to the surface decoration by the PEG shell [18]. The zeta potential represents the
274 apparent surface charge. The p722 entrapment did not modify the zeta potential compared
275 to blank LNC. LNC PEGylation decreased the zeta potential ~~from -5 mV to~~ (-29 mV and -13
276 mV) for unloaded and ~~from -6 mV to -13 mV for~~ loaded LNC (Table 1), respectively, due to
277 the electrical dipole of ethylene glycol moiety. The different suspensions have a
278 polydispersity index < 0.2, an important parameter illustrating the monodispersity of the
279 suspension. The stability of loaded LNC was assessed at 4°C (storage condition) for 3 weeks:
280 the hydrodynamic diameter, polydispersity index, zeta potential, entrapment encapsulation
281 and drug loading were not modified (Fig.S1A-C).

282

283 *Ferrocifen activity on melanoma cell viability and cell apoptosis*

284 Free p722 had a significant cytotoxicity with an $IC_{50}$ estimated at 0.09 mg/mL (corresponding
285 to 1.68 x $10^{-4}$ M). Encapsulated p722 (p722-LNC) had the same toxicity profile as the free
286 drug ($IC_{50}$ = 0.10 mg/mL corresponding to 1.87 x $10^{-4}$ M), evidencing the capacity of LNC to
287 deliver ferrocifen into B16F10 melanoma cells without additional toxicity. In addition, for
288 blank LNC, $IC_{50}$ was significantly increased (2.90 mg/mL *i.e.* 54.16 x $10^{-4}$ M) compared to free
289 or encapsulated p722 (Fig. 2A).

290 As shown in Fig. 2B, the Western blot analysis revealed that Bax, pro-caspase 9, cleaved
291 caspase 9 and pro-caspase 3 were found at higher levels in B16F10 cells under free p722
292 exposure compared with untreated cells. Furthermore, in these experimental conditions, no
293 difference in cleaved caspase 3 expression has been observed in cells treated with free p722
294 in comparison to untreated cells. This same experiment was carried out with p722-pegylated
295 LNC. No modification in the expression of Bcl2, Bax and cleaved caspase 3 was
296 demonstrated. However, an increase of pro-caspase 9, cleaved caspase 9 and pro-caspase 3
297 was found in comparison with untreated cells. ~~Furthermore, no modification of expression~~
298 ~~of the different proteins was shown in the presence of pegylated LNC without p722 (Fig. 3B).~~
299
300 *Anti-tumor efficacy of ferrocifens on a mouse model of melanoma*
301 Due to the absence of a significant difference in the volumes of tumors isolated from treated
302 mice, an analysis of the growth rate was considered; the final point chosen was the critical
303 tumor volume of 2,500 $mm^3$. It was reported that this critical tumor volume was more
304 rapidly observed for mice treated with anti-CTLA4 mAb. Conversely, this critical tumor
305 volume was evolving more slowly in mice treated with p722-pegylated LNC compared to
306 mice treated with blank LNC (Fig. 3A).
307 Moreover, in mice with melanoma, treatment with p722-pegylated LNC significantly
308 improved their survival compared to mice treated with blank LNC (22 days *versus* 13 days of
309 survival, respectively) (Fig. 3B). No difference was observed for mice treated with anti-CTLA
310 mAb in comparison with blank LNC (Fig. 3C) while a significant difference was found in the
311 survival of mice treated with p722-pegylated LNC in comparison with anti-CTLA4 mAb (Fig.
312 3D).
313

314

315 *Ferrocifen loaded LNC potentiate apoptosis via the intrinsic pathway*

316 As shown in Fig. 4, no difference was found in the expression of the different proteins tested
317 both in tumors from mice treated with anti-CTLA4 mAb or anti-CTLA4 mAb and p722-
318 pegylated LNC compared to control mice. However, a significant increase in pro-caspase 9,
319 cleaved caspase 9, pro-caspase 3 and cleaved caspase 3 has been observed in tumors from
320 mice treated with p722-pegylated LNC in comparison with control mice.

321

322 *Ferrocifen loaded LNC potentiate the activation of $CD_8^+$ T lymphocytes*

323 Quantification of $CD_8^+$ T lymphocytes was conducted on mice blood samples at different
324 times (day 0, day 9 and at the end of the *in vivo* protocol). As described in Fig. 5A, no
325 difference in the percentage of $CD_8^+$ T lymphocytes was observed whatever the time and
326 treatments. No difference was found at day 0 and at the end of the protocol in the
327 percentage of activated $CD_8^+$ T lymphocytes. However, a significant increase of activated
328 $CD_8^+$ T lymphocytes has been shown, at day 9, in blood samples from mice treated with
329 p722-pegylated LNC or p722-pegylated LNC and anti-CTLA4 mAb (Fig. 5B).

330

331

## Discussion

Because numerous preclinical and clinical studies focused on the analysis of innovative combinatory therapeutic [21];[22] in melanoma therapy, the main objective of the present work is to evaluate the therapeutic properties of p722, a new promising molecule from the ferrocifen family, encapsulated in LNC, in a mouse metastatic melanoma model. Furthermore, the secondary objective is to compare the therapeutic benefits of p722-LNC with a recognized therapeutic strategy using anti-CTLA4 antibody. Interestingly, a significant improvement in the survival rate and a slower tumor growth were found with p722 loaded LNC compared to anti-CLTA4 treatment. These data were supplemented by Western blot analyzes which confirmed that p722-LNC potentiates apoptosis by enhancing the intrinsic pathway. Furthermore, treatment with p722-LNC potentiates the activation of $CD8^+$ T lymphocytes suggesting new properties for these promising encapsulated antitumor molecules.

In the ferrocifen family, the key motif is [ferrocenyl-ene-phenol] leading to the formation of ferrocenyl quinone methides by oxidation on cancer cells. ~~Chemically, this new functional group behaves as a selective electrophile that can react with a variety of nucleophiles [23].~~ At the biological level, the entity offers some new perspectives, inducing very low $IC_{50}$ values, between 0.03 to 0.5 µM, on a range of cancer cells including some resistant to coordination complexes of $Pt^{2+}$ [16]. It operates by apoptosis and/or senescence. Inhibition of pluripotent cancer stem-cells by ferrociphenols has also been found. ~~The potential for multisite activity shown by these species is of interest in precluding and/or sidestepping the phenomena of resistance. The role of the iron generating production of ROS, is initiate, control and modulate a series of novel molecular events within cancer cells. The system is not operative on healthy cells [23]~~. Amongst the synthetized ferrocifens, the succinimido-

356 ferrociphenol compound p722 shows a strongest *in vitro* antiproliferative effets [24] while
357 its *in vivo* behavior has not been evaluated so far. The exceptional antitumoral effect of this
358 new derivative is related to the succinimide function, allowing an unprecedented
359 stabilization of the transient quinone methide, *via* an interaction between the lone pair of
360 one carbonyl of the heterocycle and the center of the aromatic quinone methide ring
361 [16,24].
362 Considering the poor water-soluble property of ferrocifens, LNC represents a suitable drug
363 delivery system thanks to its oily core [25]. Furthermore, encapsulation of ferrocifens
364 enhances cellular and tumor delivery which represents an important challenge to treat
365 cancer. ~~Thus, previous studies on LNC encapsulating ferrocifens demonstrated the efficient~~
366 ~~encapsulation and the therapeutic benefits to treat.~~ Our results confirm and improve
367 previous findings conducted on glioblastoma [26] or melanoma [10] cells, especially
368 concerning the characterization of nanovectors: as shown in Table 1, encapsulation
369 efficiency, mean size, zeta potential data are consistent with formerly cited studies and
370 these characteristics are stable over time, sustaining that these vectors are well adapted for
371 the protocols conducted on mice models.
372 Several studies evaluated the cytotoxicity of ferrocifen derivatives in various tumor cell
373 models. Thus, in a previous study, it was reported that P5 and DP1, two ferrociphenol
374 derivatives, exerted growth inhibitory effects, mainly *via* senescence, between 0.5 and 10
375 µM against Hs683 and U373 human glioma cells or B16F10 mice melanoma cells [9].
376 Furthermore, other experiments were conducted on triple-negative MDA-MB-231 breast
377 cancer cells for which an antiproliferative activity of ferrocifens was shown for an $IC_{50}$ of 2.6
378 µM [27] and 2 µM [12]. Moreover, in a study conducted on SK-Mel28 human melanoma
379 cells, $IC_{50}$ was 300 nM for ferrociphenol and 1.2 mM for ansa-ferrociphenol [28] while on 9L

rat gliosarcoma cells, the $IC_{50}$ was 0.4 and 0.6 µM for free ferrociphenol or ferrociphenol-LNC, respectively [29]. Taken together, these findings confirm a better sensitivity for p722 ferrocifen derivatives since the present study shows lower $IC_{50}$ (168 and 187 nM for free p722 and p722-LNC, respectively) compared to previous studies. This improved sensitivity justifies the use of encapsulated p722 at lower doses, than those used in the previous studies, which will ultimately limit the toxicity.

Both *in vitro* and *in vivo* studies confirm that encapsulated p722 is able to induce apoptosis on B16F10 cells by potentiating the intrinsic pathway. Several *stimuli*, including ROS, are able to regulate apoptosis of tumor cells. Thus, as previously described, ferrocifens increase the levels of ROS in tumor cells [13] and then, could induce apoptosis. ~~Due to their reactive potential, ROS can oxidize bases, leading to DNA strand breaks, intra-strand adducts, crosslinks and mutations [30]. ROS can affect the integrity of proteins and/or lipids in membranes, decreasing the fluidity and increasing membrane permeability as well as in mitochondria [31].~~ Mitochondrial dysfunction, characterized by loss of transmembrane potential and opening of mitochondrial permeability transition pores occurs *via* many apoptotic *stimuli* [32]. Ferrocifen derivatives cause disruption of $\Delta\Psi$min breast cancer cells [13]. In melanoma, the impairment of mitochondrial membrane permits the release of cytochrome *c*, an event known to occur after externalization of phosphatidylserine [33], triggering the apoptotic intrinsic pathway with activation of caspase 9 and 3 [31]. Thus, taken together, these data suggest that the increase in caspase expression and activity, showed in this study, could be explained by an enhancement of oxidative stress induced by p722.

Numerous clinical studies [34] or pre-clinical models using several tumor cell lines of solid cancers [35,36] reveal that the combination of chemotherapy and immunotherapy enhances

survival. In metastatic melanoma, it is manifest that the combination of radiotherapy with ipilimumab (human anti-CTLA4) increases the median survival of 4 to 5 months and response rates of 25.7% *versus* 6.5% (in patients treated with ipilimumab alone) [15]. Based on these data, a part of this study aims to highlight the possible beneficial effects of a combination of anti-CTLA4 mAb and p722-LNC. We purposely chose the B16F10 model and settings of high tumor challenge ~~or delayed vaccination~~ in hopes of observing cooperative effects between blockades of multiple pathways. Yet, we are surprised that, even with double blockade, we are unable to observe any significant additive effects of these molecules in the context of metastatic melanoma: anti-CTLA4 mAb is not active in this mice model while p722-LNC has a significant therapeutic interest.

Interestingly, we confirm that p722-LNC is able to improve survival of treated mice by inducing both antitumoral effect and activation of $CD8^+$ T lymphocytes. While the pro-apoptotic properties of many ferrocifens are known [23], we identify for the first time an immune-preventative approach for p722-LNC, as it has been previously proposed ~~. A possible immunogenic cell death has been postulated with ferrocifens~~ [37]. Furthermore, these properties have been suggested with hydroxytamoxifen for which an increase of activation of Jurkat-T-cells has been shown. In this cellular model, an upregulation of cell surface markers CD28, CD69 and CD5 has been reported in hydroxytamoxifen-treated cells [38]. In the present study, a synergistic effect could explain the beneficial properties of p722. After 9 days of treatment with p722-LNC, apoptosis induced by ferrocifens could enhance the release of tumor antigens activating $CD8^+$ T lymphocytes [39] *via* antigen presenting cells. Thus, $CD8^+$ T lymphocytes could either have a direct cytotoxic activity or could constitute a pool of $CD8^+$ T memory lymphocytes explaining the significant improvement in mice survival treated with p722 [40]. Moreover, p722-LNC therapy could result in increasing

428 tumor infiltration of T cells and enhanced production of cytokines associated with cytotoxic
429 T-cell function [41]. However, the precise mechanisms associated with the synergistic effects
430 observed in the present study are not fully characterized, and mechanistic studies will be
431 required to identify the role of different cellular subsets in the generation of effective
432 antitumor immunity. Overall, our findings illustrate an original approach to treat metastatic
433 melanoma through a dual property: pro-apoptotic properties and $CD8^+$ T lymphocytes
434 activation.
435 These properties are identified for p722-loaded-LNC, a promising antitumor strategy.
436 According to our data, p722 is able, on its own, to prevent the development of metastatic
437 melanoma and to improve the survival of treated mice. However, it is important to note that
438 the optimal schedule and dose to improve median survival in these murine models are not
439 directly transposable in studies in humans, herein suggesting further preclinical (in other
440 animal models) and clinical studies.
441
442 **Acknowledgments**
443 The authors wish to thank the Maine et Loire League against Cancer* for its financial support
444 in the realization of this project. Furthermore, the authors would like to thank the French
445 Dermatology Society for the financing of the Master program of STR. The authors thank Ms
446 Camille Farrell Robert and Ms Isabelle Brunois-Debus for their careful editing.
447 *Comité départemental du Maine et Loire de la Ligue contre le Cancer
448
449

450 **References**


451 1. Ossio, R.; Roldán-Marín, R.; Martínez-Said, H.; Adams, D.J.; Robles-Espinoza, C.D.
452 Melanoma: a global perspective. *Nat Rev Cancer* **2017**, *17*, 393-394,
453 doi:10.1038/nrc.2017.43.

454 2. Garbe, C.; Peris, K.; Hauschild, A.; Saiag, P.; Middleton, M.; Bastholt, L.; Grob, J.J.;
455 Malvehy, J.; Newton-Bishop, J.; Stratigos, A.J., et al. Diagnosis and treatment of melanoma.
456 European consensus-based interdisciplinary guideline - Update 2016. *Eur J Cancer* **2016**, *63*,
457 201-217, doi:10.1016/j.ejca.2016.05.005.

458 3. Michot, J.M.; Bigenwald, C.; Champiat, S.; Collins, M.; Carbonnel, F.; Postel-Vinay, S.;
459 Berdelou, A.; Varga, A.; Bahleda, R.; Hollebecque, A., et al. Immune-related adverse events
460 with immune checkpoint blockade: a comprehensive review. *Eur J Cancer* **2016**, *54*, 139-148,
461 doi:10.1016/j.ejca.2015.11.016.

462 4. Tivol, E.A.; Borriello, F.; Schweitzer, A.N.; Lynch, W.P.; Bluestone, J.A.; Sharpe, A.H.
463 Loss of CTLA-4 leads to massive lymphoproliferation and fatal multiorgan tissue destruction,
464 revealing a critical negative regulatory role of CTLA-4. *Immunity* **1995**, *3*, 541-547,
465 doi:10.1016/1074-7613(95)90125-6.

466 5. Hughes, T.; Klairmont, M.; Sharfman, W.H.; Kaufman, H.L. Interleukin-2, Ipilimumab,
467 and Anti-PD-1: Clinical Management and the Evolving Role of Immunotherapy for the
468 Treatment of Patients With Metastatic Melanoma. *Cancer Biol Ther* **2015**, 0,
469 doi:10.1080/15384047.2015.1095401.

470 6. Lorentzen, H.F. Targeted therapy for malignant melanoma. *Curr Opin Pharmacol*
471 **2019**, *46*, 116-121, doi:10.1016/j.coph.2019.05.010.

472 7. Hodi, F.S.; O'Day, S.J.; McDermott, D.F.; Weber, R.W.; Sosman, J.A.; Haanen, J.B.;
473 Gonzalez, R.; Robert, C.; Schadendorf, D.; Hassel, J.C., et al. Improved survival with

474 ipilimumab in patients with metastatic melanoma. *N Engl J Med* **2010**, *363*, 711-723,
475 doi:10.1056/NEJMoa1003466.
476 8. Paulson, K.G.; Lahman, M.C.; Chapuis, A.G.; Brownell, I. Immunotherapy for skin
477 cancer. *Int Immunol* **2019**, *31*, 465-475, doi:10.1093/intimm/dxz012.
478 9. Bruyère, C.; Mathieu, V.; Vessières, A.; Pigeon, P.; Top, S.; Jaouen, G.; Kiss, R.
479 Ferrocifen derivatives that induce senescence in cancer cells: selected examples. *J Inorg*
480 *Biochem* **2014**, *141*, 144-151, doi:10.1016/j.jinorgbio.2014.08.015.
481 10. Resnier, P.; Galopin, N.; Sibiril, Y.; Clavreul, A.; Cayon, J.; Briganti, A.; Legras, P.;
482 Vessières, A.; Montier, T.; Jaouen, G., et al. Efficient ferrocifen anticancer drug and Bcl-2
483 gene therapy using lipid nanocapsules on human melanoma xenograft in mouse. *Pharmacol*
484 *Res* **2017**, *126*, 54-65, doi:10.1016/j.phrs.2017.01.031.
485 11. Michard, Q.; Jaouen, G.; Vessieres, A.; Bernard, B.A. Evaluation of cytotoxic
486 properties of organometallic ferrocifens on melanocytes, primary and metastatic melanoma
487 cell lines. *J Inorg Biochem* **2008**, *102*, 1980-1985, doi:10.1016/j.jinorgbio.2008.07.014.
488 12. Lainé, A.L.; Adriaenssens, E.; Vessières, A.; Jaouen, G.; Corbet, C.; Desruelles, E.;
489 Pigeon, P.; Toillon, R.A.; Passirani, C. The in vivo performance of ferrocenyl tamoxifen lipid
490 nanocapsules in xenografted triple negative breast cancer. *Biomaterials* **2013**, *34*, 6949-
491 6956, doi:10.1016/j.biomaterials.2013.05.065.
492 13. Lu, C.; Heldt, J.M.; Guille-Collignon, M.; Lemaître, F.; Jaouen, G.; Vessières, A.;
493 Amatore, C. Quantitative analyses of ROS and RNS production in breast cancer cell lines
494 incubated with ferrocifens. *ChemMedChem* **2014**, *9*, 1286-1293,
495 doi:10.1002/cmdc.201402016.

496 14. Allard, E.; Huynh, N.T.; Vessières, A.; Pigeon, P.; Jaouen, G.; Benoit, J.P.; Passirani, C.
497 Dose effect activity of ferrocifen-loaded lipid nanocapsules on a 9L-glioma model. *Int J*
498 *Pharm* **2009**, *379*, 317-323, doi:10.1016/j.ijpharm.2009.05.031.
499 15. Koller, K.M.; Mackley, H.B.; Liu, J.; Wagner, H.; Talamo, G.; Schell, T.D.; Pameijer, C.;
500 Neves, R.I.; Anderson, B.; Kokolus, K.M., et al. Improved survival and complete response
501 rates in patients with advanced melanoma treated with concurrent ipilimumab and
502 radiotherapy versus ipilimumab alone. *Cancer Biol Ther* **2017**, *18*, 36-42,
503 doi:10.1080/15384047.2016.1264543.
504 16. Pigeon, P.; Wang, Y.; Top, S.; Najlaoui, F.; Garcia Alvarez, M.C.; Bignon, J.;
505 McGlinchey, M.J.; Jaouen, G. A New Series of Succinimido-ferrociphenols and Related
506 Heterocyclic Species Induce Strong Antiproliferative Effects, Especially against Ovarian
507 Cancer Cells Resistant to Cisplatin. *J Med Chem* **2017**, *60*, 8358-8368,
508 doi:10.1021/acs.jmedchem.7b00743.
509 17. Heurtault, B.; Saulnier, P.; Pech, B.; Proust, J.E.; Benoit, J.P. A novel phase inversion-
510 based process for the preparation of lipid nanocarriers. *Pharm Res* **2002**, *19*, 875-880.
511 18. Perrier, T.; Saulnier, P.; Fouchet, F.; Lautram, N.; Benoît, J.P. Post-insertion into Lipid
512 NanoCapsules (LNCs): From experimental aspects to mechanisms. *Int J Pharm* **2010**, *396*,
513 204-209, doi:10.1016/j.ijpharm.2010.06.019.
514 19. Morille, M.; Montier, T.; Legras, P.; Carmoy, N.; Brodin, P.; Pitard, B.; Benoît, J.P.;
515 Passirani, C. Long-circulating DNA lipid nanocapsules as new vector for passive tumor
516 targeting. *Biomaterials* **2010**, *31*, 321-329, doi:10.1016/j.biomaterials.2009.09.044.
517 20. Bastiat, G.; Pritz, C.O.; Roider, C.; Fouchet, F.; Lignières, E.; Jesacher, A.; Glueckert, R.;
518 Ritsch-Marte, M.; Schrott-Fischer, A.; Saulnier, P., et al. A new tool to ensure the fluorescent

519 dye labeling stability of nanocarriers: a real challenge for fluorescence imaging. *J Control*
520 *Release* **2013**, *170*, 334-342, doi:10.1016/j.jconrel.2013.06.014.
521 21. Zimmer, L.; Apuri, S.; Eroglu, Z.; Kottschade, L.A.; Forschner, A.; Gutzmer, R.; Schlaak,
522 M.; Heinzerling, L.; Krackhardt, A.M.; Loquai, C., et al. Ipilimumab alone or in combination
523 with nivolumab after progression on anti-PD-1 therapy in advanced melanoma. *Eur J Cancer*
524 **2017**, *75*, 47-55, doi:10.1016/j.ejca.2017.01.009.
525 22. Wolchok, J.D.; Chiarion-Sileni, V.; Gonzalez, R.; Rutkowski, P.; Grob, J.J.; Cowey, C.L.;
526 Lao, C.D.; Wagstaff, J.; Schadendorf, D.; Ferrucci, P.F., et al. Overall Survival with Combined
527 Nivolumab and Ipilimumab in Advanced Melanoma. *N Engl J Med* **2017**, *377*, 1345-1356,
528 doi:10.1056/NEJMoa1709684.
529 23. Jaouen, G.; Vessières, A.; Top, S. Ferrocifen type anti cancer drugs. *Chem Soc Rev*
530 **2015**, *44*, 8802-8817, doi:10.1039/c5cs00486a.
531 24. Wang, Y.; Pigeon, P.; Top, S.; Sanz García, J.; Troufflard, C.; Ciofini, I.; McGlinchey,
532 M.J.; Jaouen, G. Atypical Lone Pair-π Interaction with Quinone Methides in a Series of Imido-
533 Ferrociphenol Anticancer Drug Candidates. *Angew Chem Int Ed Engl* **2019**, *58*, 8421-8425,
534 doi:10.1002/anie.201902456.
535 25. Lainé, A.L.; Clavreul, A.; Rousseau, A.; Tétaud, C.; Vessieres, A.; Garcion, E.; Jaouen,
536 G.; Aubert, L.; Guilbert, M.; Benoit, J.P., et al. Inhibition of ectopic glioma tumor growth by a
537 potent ferrocenyl drug loaded into stealth lipid nanocapsules. *Nanomedicine* **2014**, *10*, 1667-
538 1677, doi:10.1016/j.nano.2014.05.002.
539 26. Karim, R.; Lepeltier, E.; Esnault, L.; Pigeon, P.; Lemaire, L.; Lépinoux-Chambaud, C.;
540 Clere, N.; Jaouen, G.; Eyer, J.; Piel, G., et al. Enhanced and preferential internalization of lipid
541 nanocapsules into human glioblastoma cells: effect of a surface-functionalizing NFL peptide.
542 *Nanoscale* **2018**, *10*, 13485-13501, doi:10.1039/c8nr02132e.

543 27. Cázares-Marinero, J.e.J.; Top, S.; Vessières, A.; Jaouen, G. Synthesis and
544 antiproliferative activity of hydroxyferrocifen hybrids against triple-negative breast cancer
545 cells. *Dalton Trans* **2014**, *43*, 817-830, doi:10.1039/c3dt52070f.
546 28. Resnier, P.; LeQuinio, P.; Lautram, N.; André, E.; Gaillard, C.; Bastiat, G.; Benoit, J.P.;
547 Passirani, C. Efficient in vitro gene therapy with PEG siRNA lipid nanocapsules for passive
548 targeting strategy in melanoma. *Biotechnol J* **2014**, *9*, 1389-1401,
549 doi:10.1002/biot.201400162.
550 29. Laine, A.L.; Huynh, N.T.; Clavreul, A.; Balzeau, J.; Béjaud, J.; Vessieres, A.; Benoit, J.P.;
551 Eyer, J.; Passirani, C. Brain tumour targeting strategies via coated ferrociphenol lipid
552 nanocapsules. *Eur J Pharm Biopharm* **2012**, *81*, 690-693, doi:10.1016/j.ejpb.2012.04.012.
553 30. Murata, M. Inflammation and cancer. *Environ Health Prev Med* **2018**, *23*, 50,
554 doi:10.1186/s12199-018-0740-1.
555 31. Obrador, E.; Liu-Smith, F.; Dellinger, R.W.; Salvador, R.; Meyskens, F.L.; Estrela, J.M.
556 Oxidative stress and antioxidants in the pathophysiology of malignant melanoma. *Biol Chem*
557 **2019**, *400*, 589-612, doi:10.1515/hsz-2018-0327.
558 32. Kroemer, G.; Galluzzi, L.; Vandenabeele, P.; Abrams, J.; Alnemri, E.S.; Baehrecke, E.H.;
559 Blagosklonny, M.V.; El-Deiry, W.S.; Golstein, P.; Green, D.R., et al. Classification of cell death:
560 recommendations of the Nomenclature Committee on Cell Death 2009. *Cell Death Differ*
561 **2009**, *16*, 3-11, doi:10.1038/cdd.2008.150.
562 33. Ford, W.E.; Ren, W.; Blackmore, P.F.; Schoenbach, K.H.; Beebe, S.J. Nanosecond
563 pulsed electric fields stimulate apoptosis without release of pro-apoptotic factors from
564 mitochondria in B16f10 melanoma. *Arch Biochem Biophys* **2010**, *497*, 82-89,
565 doi:10.1016/j.abb.2010.03.008.

566 34. Arriola, E.; Wheater, M.; Galea, I.; Cross, N.; Maishman, T.; Hamid, D.; Stanton, L.;
567 Cave, J.; Geldart, T.; Mulatero, C., et al. Outcome and Biomarker Analysis from a Multicenter
568 Phase 2 Study of Ipilimumab in Combination with Carboplatin and Etoposide as First-Line
569 Therapy for Extensive-Stage SCLC. *J Thorac Oncol* **2016**, *11*, 1511-1521,
570 doi:10.1016/j.jtho.2016.05.028.
571 35. Fritz, J.; Karakhanova, S.; Brecht, R.; Nachtigall, I.; Werner, J.; Bazhin, A.V. In vitro
572 immunomodulatory properties of gemcitabine alone and in combination with interferon-
573 alpha. *Immunol Lett* **2015**, *168*, 111-119, doi:10.1016/j.imlet.2015.09.017.
574 36. Jure-Kunkel, M.; Masters, G.; Girit, E.; Dito, G.; Lee, F.; Hunt, J.T.; Humphrey, R.
575 Synergy between chemotherapeutic agents and CTLA-4 blockade in preclinical tumor
576 models. *Cancer Immunol Immunother* **2013**, *62*, 1533-1545, doi:10.1007/s00262-013-1451-5.
577 37. Terenzi, A.; Pirker, C.; Keppler, B.K.; Berger, W. Anticancer metal drugs and
578 immunogenic cell death. *J Inorg Biochem* **2016**, *165*, 71-79,
579 doi:10.1016/j.jinorgbio.2016.06.021.
580 38. Chlichlia, K.; Moldenhauer, G.; Daniel, P.T.; Busslinger, M.; Gazzolo, L.; Schirrmacher,
581 V.; Khazaie, K. Immediate effects of reversible HTLV-1 tax function: T-cell activation and
582 apoptosis. *Oncogene* **1995**, *10*, 269-277.
583 39. Palucka, A.K.; Coussens, L.M. The Basis of Oncoimmunology. *Cell* **2016**, *164*, 1233-
584 1247, doi:10.1016/j.cell.2016.01.049.
585 40. Ho, P.C.; Bihuniak, J.D.; Macintyre, A.N.; Staron, M.; Liu, X.; Amezquita, R.; Tsui, Y.C.;
586 Cui, G.; Micevic, G.; Perales, J.C., et al. Phosphoenolpyruvate Is a Metabolic Checkpoint of
587 Anti-tumor T Cell Responses. *Cell* **2015**, *162*, 1217-1228, doi:10.1016/j.cell.2015.08.012.
588 41. Wu, L.; Yun, Z.; Tagawa, T.; Rey-McIntyre, K.; de Perrot, M. CTLA-4 blockade expands
589 infiltrating T cells and inhibits cancer cell repopulation during the intervals of chemotherapy

590 in murine mesothelioma. *Mol Cancer Ther* **2012**, *11*, 1809-1819, doi:10.1158/1535-
591 7163.MCT-11-1014.

592 **Legends**

593 **Table 1**

594 Physico-chemical parameters and encapsulation yield of p722-LNC

595

596 **Figure 1**

597 Chemical structure of p722

598 **Figure 2**

599 Cytotoxicity of free p722, p722-loaded LNC on B16F10 melanoma cell line (A). Evaluation of
600 B16F10 cell viability by MTT assay, n=3. (B) Pro-apoptotic properties of free p722, blank LNC
601 and p722-LNC on B16F10 melanoma cell line. Evaluation of Bcl2, Bax, procaspase 9, cleaved
602 caspase 9, procaspase 3 and cleaved caspase 3, n=3 * $p<0.05$

603 **Figure 3**

604 Efficacy evaluation of p722-LNC and comparison with anti-CTLA4 mAb treatment on B16F10
605 mice-xenografted model. (A). Evaluation of the survival of mice treated with p722-LNC
606 compared to mice treated with blank LNC, n=6 *$p=0.013$ (B). Evaluation of the mice survival
607 treated with anti-CTLA4 mAb compared to mice treated with blank LNC, n=6 (C). Evaluation
608 of the survival of mice treated with p722-LNC compared to mice treated with anti-CTLA4
609 mAb, n=6 *$p=0.012$

610 **Figure 4**

611 Pro-apoptotic properties of p722-LNC. Western blot evaluation of Bcl2, Bax, procaspase 9,
612 cleaved caspase 9, procaspase 3, cleaved caspase 3 expression, n=3. Table represents the

613 ratio between the expression of studied proteins and the expression of β-actin. (a)

614 significant results compared to control mice ($p<0.05$).

615 **Figure 5**

616 p722-LNC activates $CD8^+$ T lymphocytes from mice tumor at day 9. (A) Evaluation of the

617 percentage expression of $CD8^+$ T lymphocytes at day 0, day 9 and at the end of the protocol,

618 n=6. (B) Evaluation of the percentage expression of $CD8^+$ activated T lymphocytes at D0, D9

619 and at the end of the protocol, n=6 * $p<0.05$.

**Figure 1**

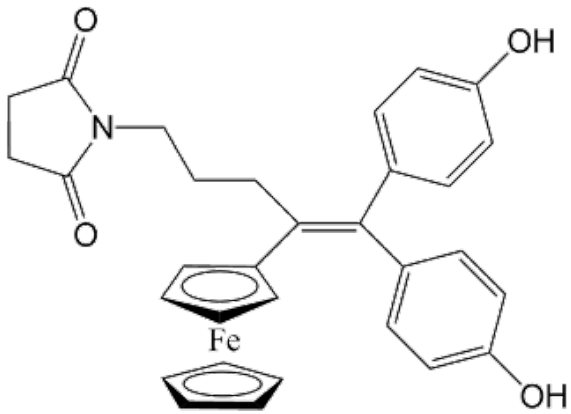

**Figure 2**

**A**

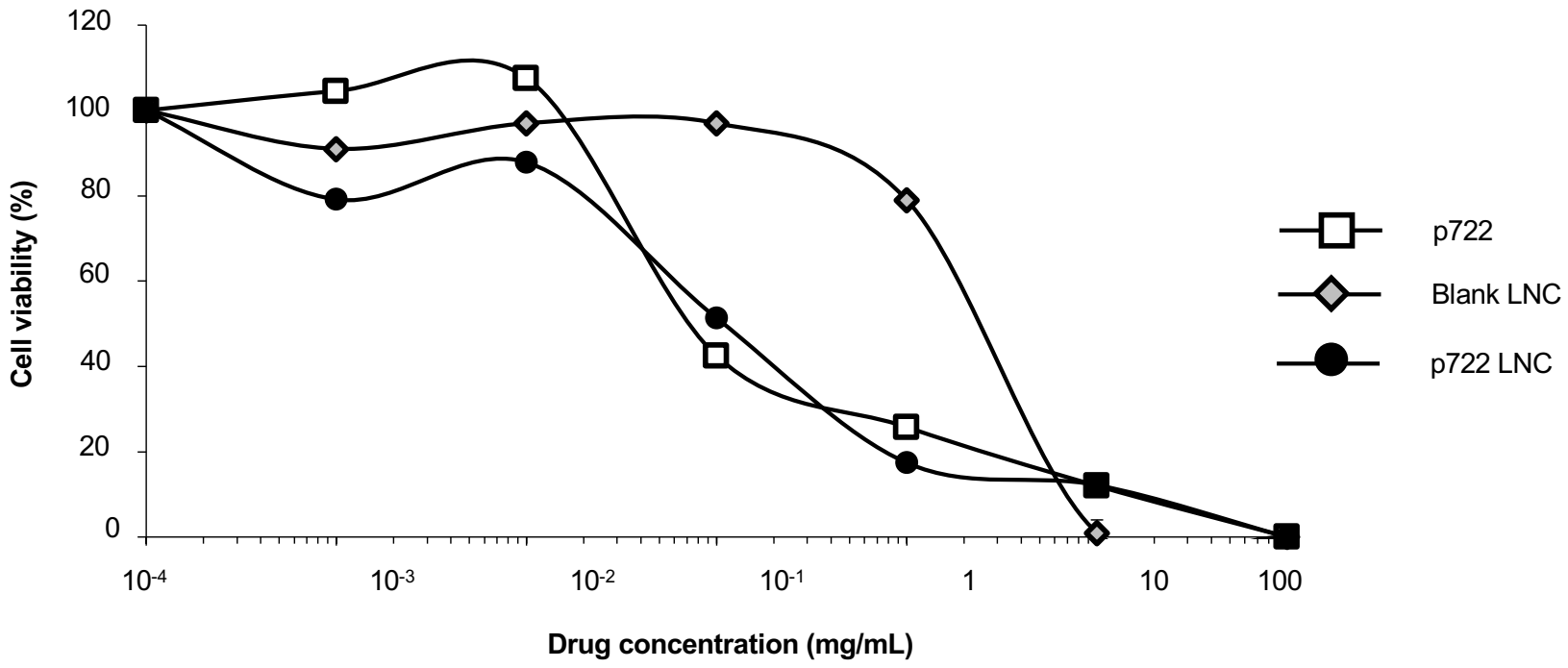


| | IC50 (mg/mL) | IC50 (M) |
|---|---|---|
| p722 | 0.09 | $1.68 \times 10^{-7}$ |
| Blank LNC | 2.90 | $54.16 \times 10^{-7}$ |
| p722 LNC | 0.10 | $1.87 \times 10^{-7}$ |

## Figure 2

**B**

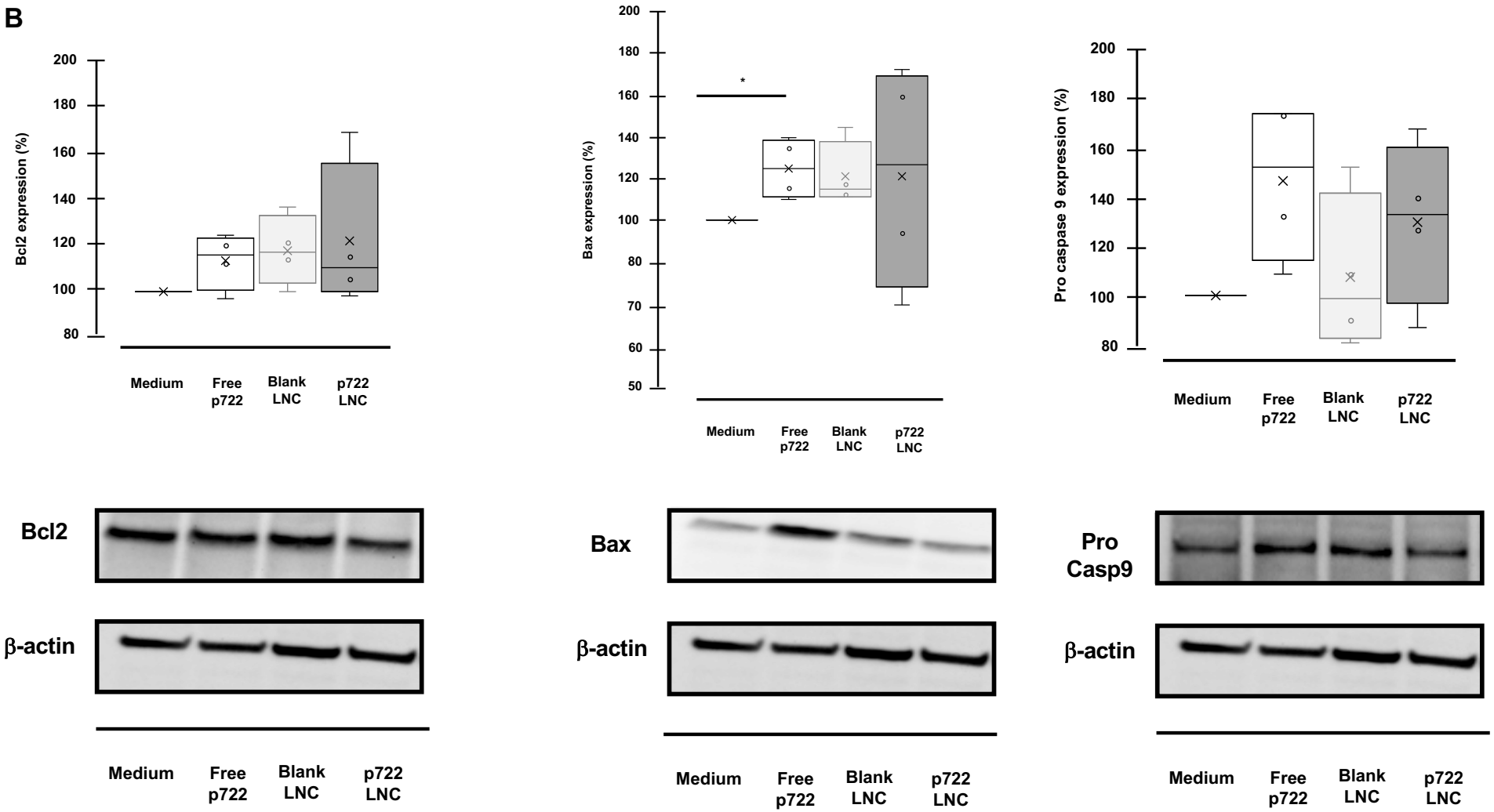
Bcl2 expression (%)
200
180
160
140
120
100
80
Medium
Free p722
Blank LNC
p722 LNC
Bax expression (%)
200
180
160
140
120
100
80
70
60
50
*
Medium
Free p722
Blank LNC
p722 LNC
Pro caspase 9 expression (%)
200
180
160
140
120
100
80
Medium
Free p722
Blank LNC
p722 LNC
Bcl2
β-actin
Medium
Free p722
Blank LNC
p722 LNC
Bax
β-actin
Medium
Free p722
Blank LNC
p722 LNC
Pro Casp9
β-actin
Medium
Free p722
Blank LNC
p722 LNC

## Figure 2

**B**

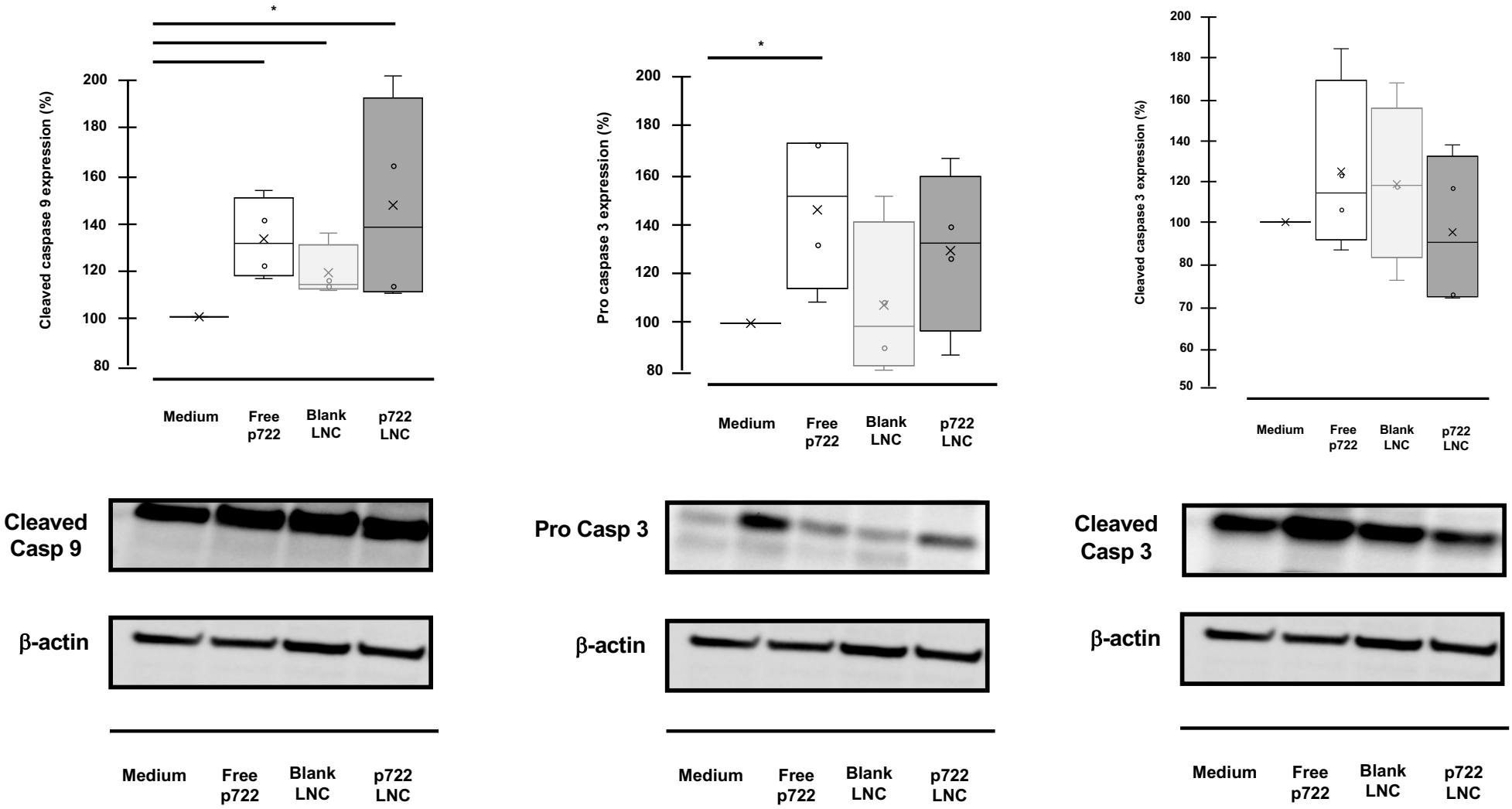
*
Cleaved caspase 9 expression (%)
200
180
160
140
120
100
80
Medium
Free p722
Blank LNC
p722 LNC
*
Pro caspase 3 expression (%)
200
180
160
140
120
100
80
Medium
Free p722
Blank LNC
p722 LNC
Cleaved caspase 3 expression (%)
200
180
160
140
120
100
80
70
60
50
Medium
Free p722
Blank LNC
p722 LNC
Cleaved Casp 9
β-actin
Medium
Free p722
Blank LNC
p722 LNC
Pro Casp 3
β-actin
Medium
Free p722
Blank LNC
p722 LNC
Cleaved Casp 3
β-actin
Medium
Free p722
Blank LNC
p722 LNC

Figure 3

A

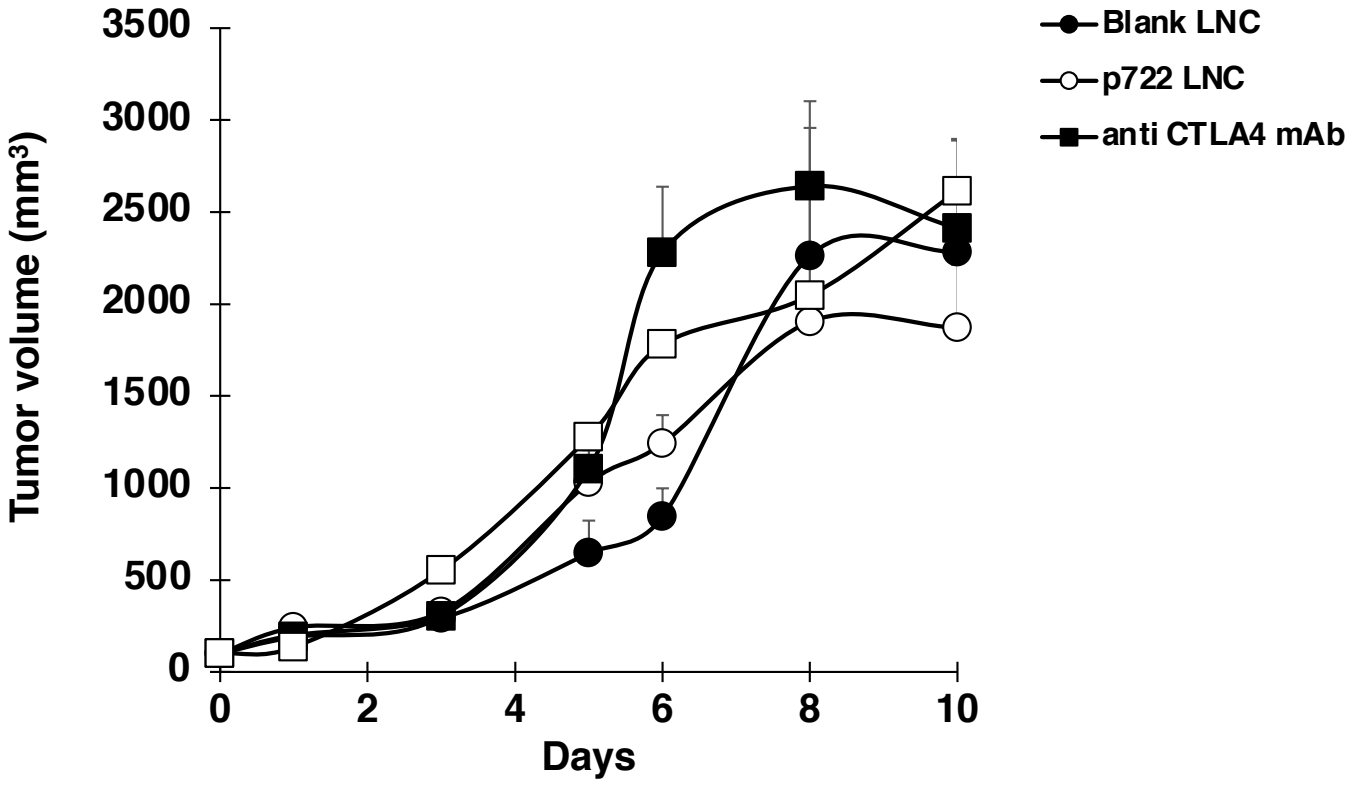
3500
3000
2500
2000
1500
1000
500
0
Tumor volume (mm3)
0
2
4
6
8
10
Days
Blank LNC
p722 LNC
anti CTLA4 mAb

**Figure 3**

**B**

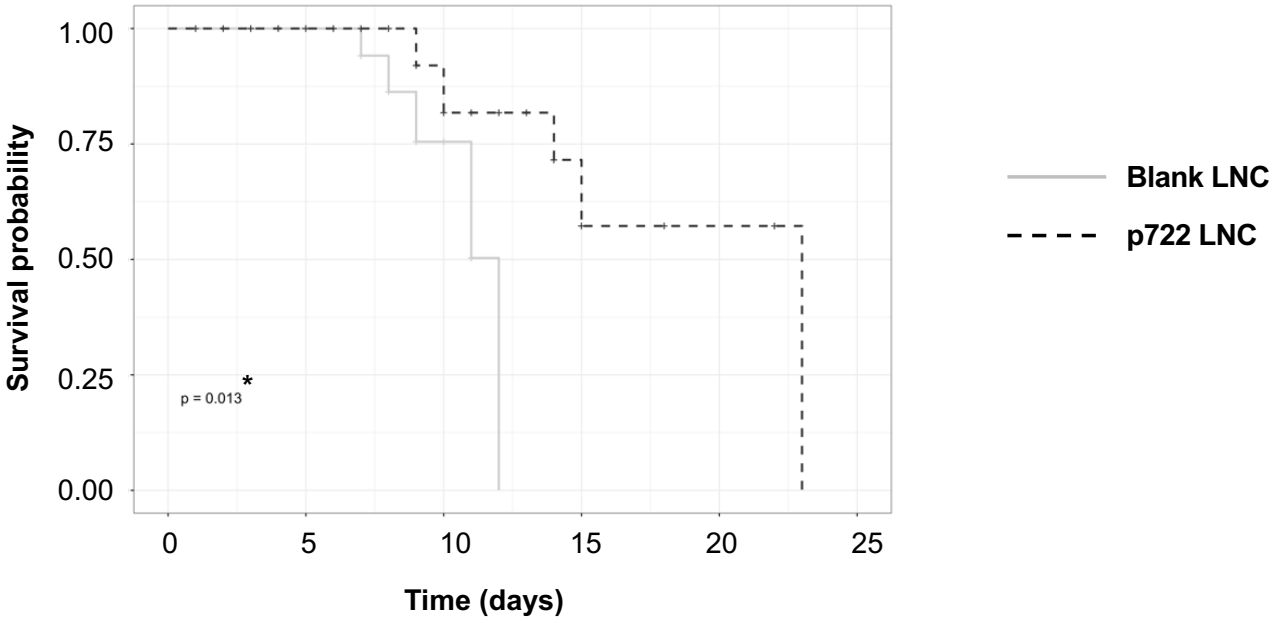
1.00
0.75
0.50
0.25
0.00
Survival probability
p = 0.013
*
0
5
10
15
20
25
Time (days)
Blank LNC
p722 LNC

**C**

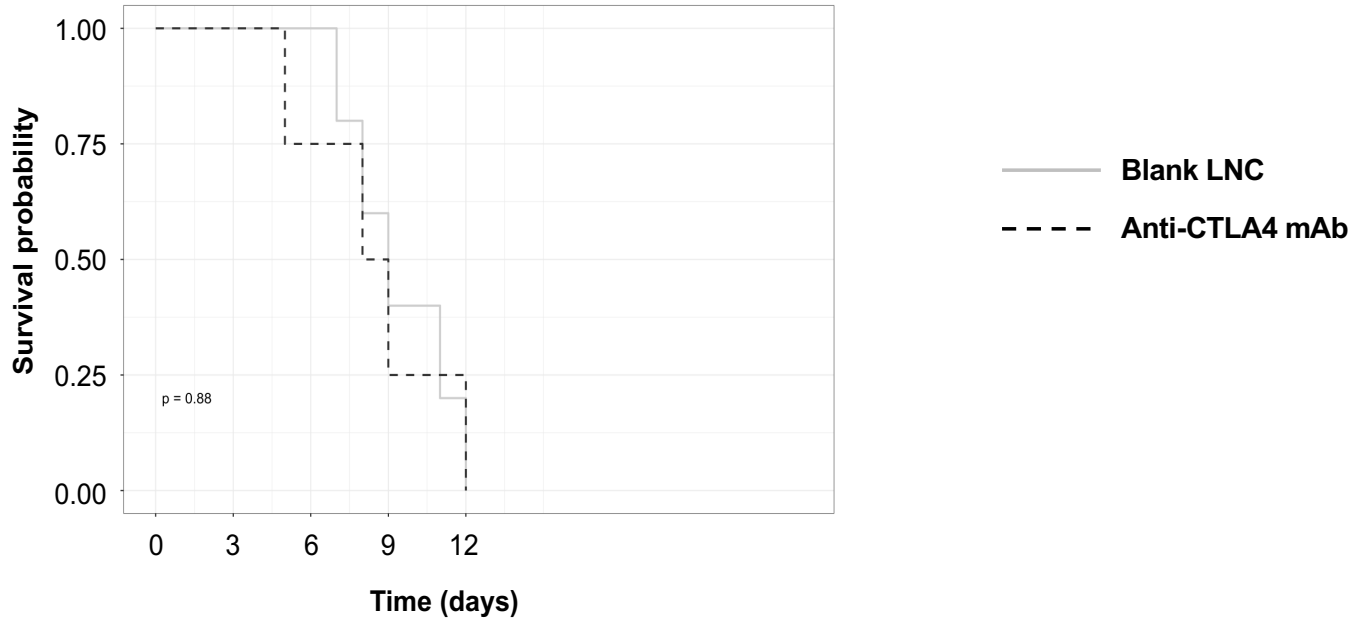
1.00
0.75
0.50
0.25
0.00
Survival probability
p = 0.88
0
3
6
9
12
Time (days)
Blank LNC
Anti-CTLA4 mAb

**Figure 3**

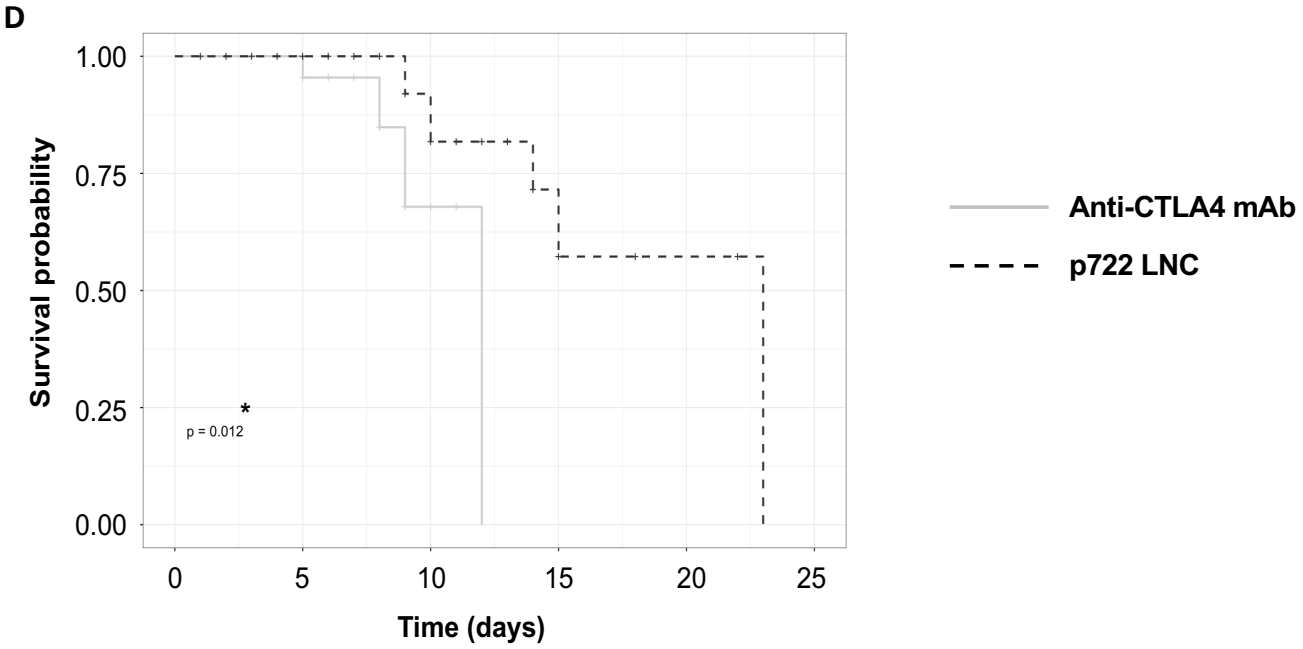
D
1.00
0.75
0.50
0.25
0.00
Survival probability
*
p = 0.012
0
5
10
15
20
25
Time (days)
Anti-CTLA4 mAb
p722 LNC

**Figure 4**

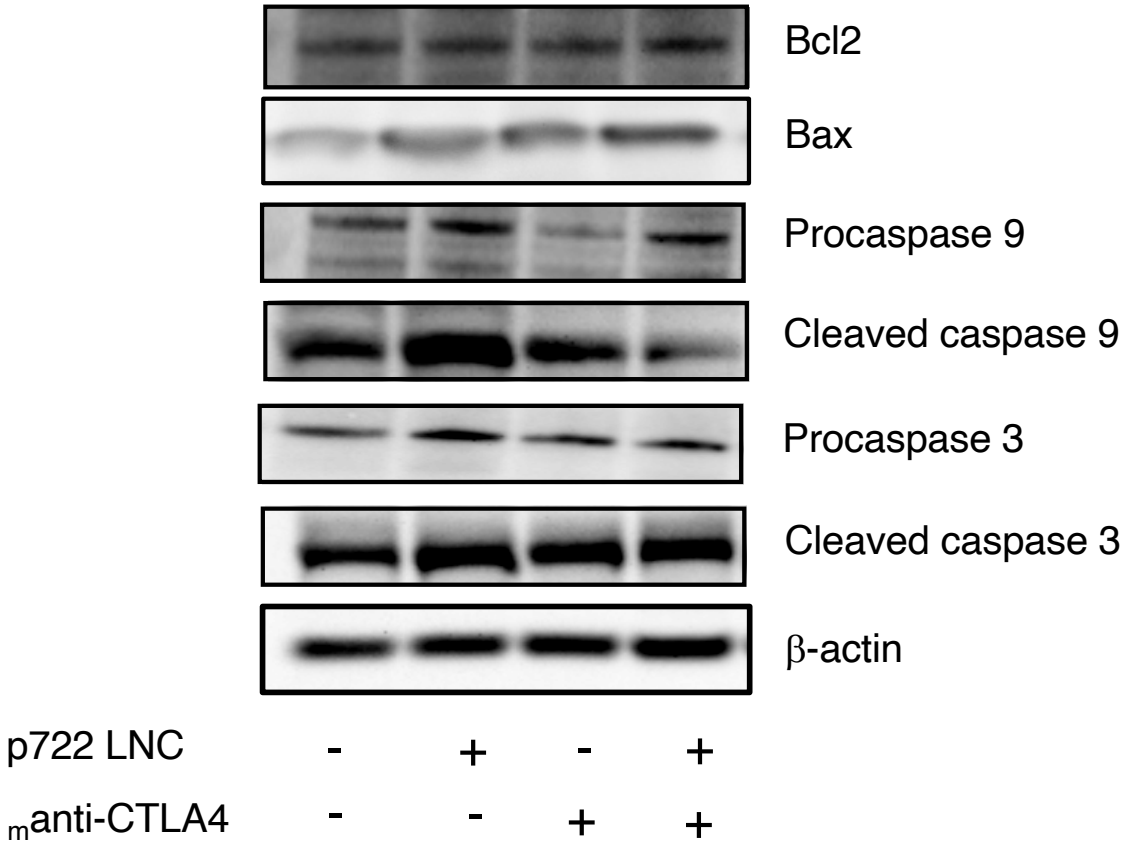


| | Control | p722 LNC | mAnti-CTLA4 | p722 LNC mAnti-CTLA4 |
|---|---|---|---|---|
| **BCl2** | 99.29 +/- 4.27 | 120.60 +/- 1.17 | 117.16 +/- 6.32 | 114.00 +/- 19.03 |
| **Bax** | 99.57 +/- 7.25 | 127.00 +/- 18.61 | 102.28 +/- 19.77 | 91.85 +/- 30.23 |
| **Procaspase 9** | 107.75 +/- 17.57 | 126.28 +/- 5.52[a] | 115.71 +/- 23.22 | 103.5 +/- 25.81 |
| **Cleaved caspase 9** | 115.25 +/- 20.41 | 171.00 +/- 17.30[a] | 95.00 +/- 19.00 | 63.66 +/- 22.81 |
| **Procaspase 3** | 86.61 +/- 6.54 | 115.00 +/- 7.22[a] | 86.66 +/- 10.92 | 98.66 +/- 16.48 |
| **Cleaved caspase 3** | 98.07 +/- 7.71 | 236.57 +/- 66.95[a] | 166.28 +/- 48.72 | 199.28 +/- 99.22 |

Figure 5

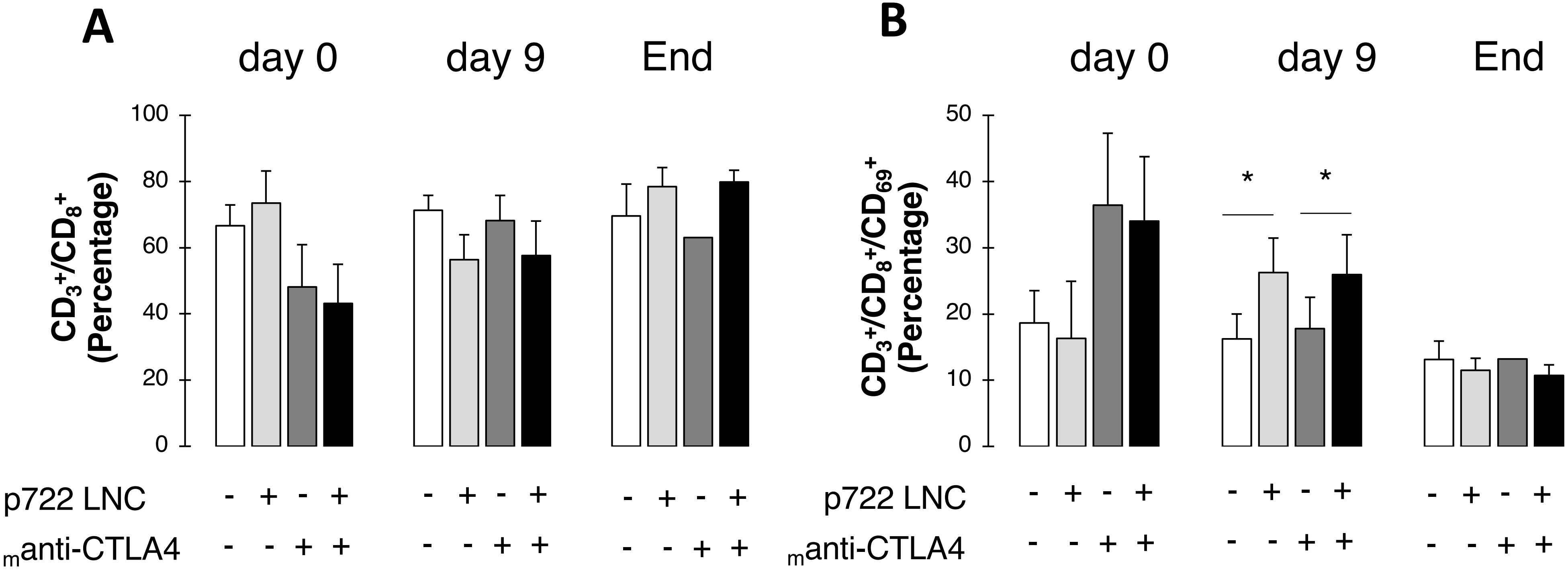

A
day 0
day 9
End
100
80
60
40
20
0
CD3+/CD8+ (Percentage)
p722 LNC
manti-CTLA4
B
day 0
day 9
End
50
40
30
20
10
0
CD3+/CD8+/CD69+ (Percentage)
*
*
p722 LNC
manti-CTLA4

**Figure S1**

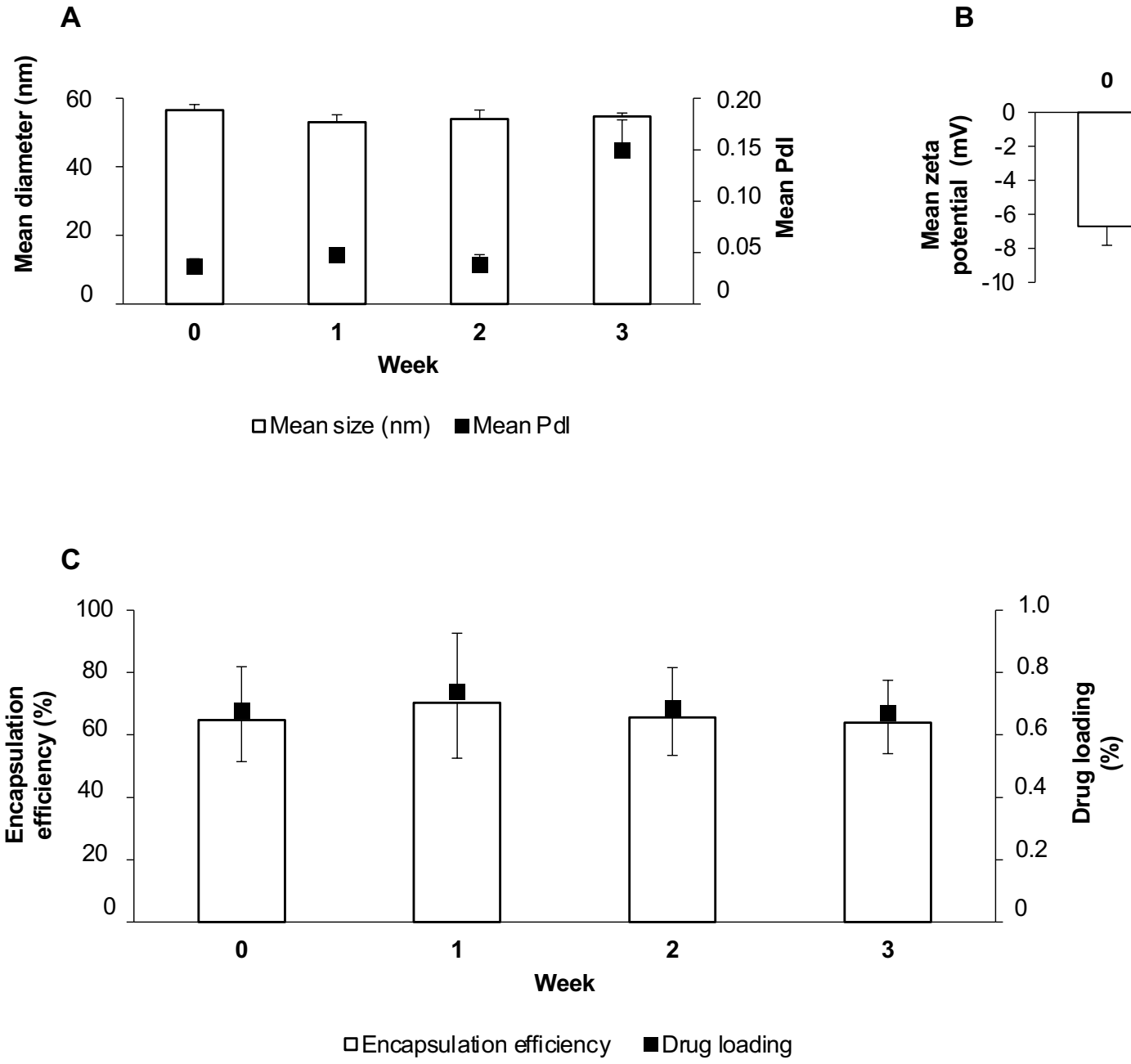
A
Mean diameter (nm)
60
40
20
0
0.20
0.15
0.10
0.05
0
Mean PdI
0
1
2
3
Week
Mean size (nm)
Mean PdI
B
Week
0
1
2
3
Mean zeta potential (mV)
0
-2
-4
-6
-8
-10
Mean zêta potential (mV)
C
Encapsulation efficiency (%)
100
80
60
40
20
0
1.0
0.8
0.6
0.4
0.2
0
Drug loading (%)
0
1
2
3
Week
Encapsulation efficiency
Drug loading

Table 1

| | Mean diameter (nm) | Mean PdI | Mean zeta potential (mV) | EE (%) | Drug loading (%) |
|---|---|---|---|---|---|
| Blank pegylated-LNC | 72.4 +/- 0.8 | 0.12 +/- 0.01 | -29.0 +/- 1.2 | / | / |
| p722 pegylated-LNC [2.25 mM] | 70.0 +/- 1.0 | 0.15 +/- 0.01 | -13.5 +/- 0.5 | 64.8 +/- 13.4 | 0.7 +/- 0.1 |

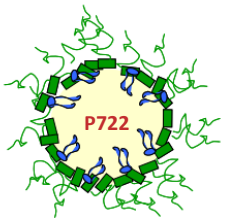


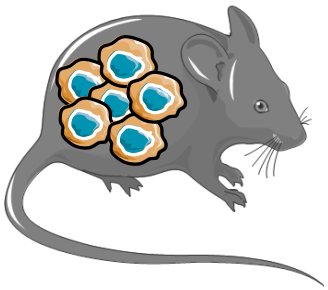

Improved mice survival

- Potentiation of intrinsic apoptotic pathway
- Activation of $CD_8^+$ T lymphocytes